# Successive convex approximation for rate maximisation in cooperative multiple-input–multiple-output-orthogonal frequency-division multiplexing systems

*Chih-yu Hsu* ✉, *Phee Lep Yeoh, Brian Scott Krongold*

*Department of Electrical and Electronic Engineering, University of Melbourne, Melbourne 3010, Victoria, Australia*
✉ *E-mail: cyhsu@student.unimelb.edu.au*

**Abstract**: In this study, the authors propose a continuous rate and power allocation algorithm for multiuser downlink multiple-input–multiple-output orthogonal frequency-division multiplexing systems with coordinated multi-point transmission. The optimisation problem is formulated as a weighted sum-rate maximisation problem subject to per-antenna power constraints across multiple cooperating base stations (BSs). The practical consideration of the per-antenna power constraint limits the average transmit antenna power which indirectly controls the inherent issue of high peak powers in OFDM. The proposed algorithm employs a successive convex approximation (SCA) technique to dynamically allocate powers to multiple co-channel user terminals. They provide a convexity proof of the transformed optimisation problem and they show that the proposed algorithm converges to a unique solution. They compare the proposed SCA algorithm with two alternative approaches: (i) iterative waterfilling (IWF) and (ii) zero-forcing beamforming (ZFB) with semi-orthogonal user selection under both per-antenna and per-BS power constraint scenarios. Their simulation results highlight that the proposed SCA algorithm outperforms the existing IWF and ZFB in noise-limited environments under both power constraint scenarios.

## 1 Introduction

Multiple-input–multiple-output (MIMO) orthogonal frequency-division multiplexing (OFDM) has been featured prominently as the broadband cellular platform for next generation LTE-advanced systems [1–3]. When perfect channel state information (CSI) is available to both transmitters and receivers, the overall throughput of MIMO-OFDM systems can be improved significantly by utilising the spatial diversity of the MIMO channel in each OFDM subchannel. Furthermore, the utilisation of each MIMO-OFDM spatial-subchannel can be optimised via dynamic resource allocation algorithms in which substantial improvements on the system performance have been demonstrated in [4, 5]. However, the intercell interference (ICI) is the limiting factor on the performance of multiuser MIMO-OFDM systems. This is particularly true at the cell-edge where user terminals (UTs) receive multiple signals from multiple base stations (BSs). For each UTs, the data throughput depends on the tradeoff between their own power and powers allocated to all other interfering UTs in the shared OFDM subchannel.

The ICI can be mitigated by utilising coordinated multi-point (CoMP) transmission techniques at multiple cooperating BSs [6, 7]. The downlink CoMP transmission technique can be classified into two main strategies; coordinated scheduling/beamforming and joint processing [8, 9]. In coordinated scheduling/beamforming, ICI is avoided by transmitting to a UT from one BS at any time. As a result, only CSI of the serving cell is shared amongst the cooperating BSs. In joint processing, ICI is mitigated by transmitting to a UT from all the cooperating BSs simultaneously. As such, both user data and CSI of all the cells are shared amongst the cooperating BSs. In this paper, we focus on the joint processing strategy in a multicell scenario, where a central processor (CP) is employed for executing our proposed resource allocation algorithm.

In addition to mitigating interference through cooperating BSs, adaptive resource allocation schemes can be employed to further improve system throughput. The resource allocation problem for downlink MIMO-OFDM systems has been studied extensively for the single-user case. In the multiuser scenario, the problem becomes mathematically challenging as the optimisation problem is non-convex in the presence of interference. As a result, the globally optimal solution is difficult to obtain efficiently. To obtain the optimal solution, a coding scheme called dirty paper coding (DPC) is proposed in [10]. The DPC employs a non-linear precoding scheme which presubtracts interference. However, DPC requires high computational demands in successive encodings and decodings which are difficult to implement in practice.

A number of suboptimal strategies for multiuser MIMO-OFDM have been proposed to solve this non-convex problem. The iterative waterfilling (IWF) approach in [11] makes the problem more tractable by treating the interference from the neighbouring cells as a noise component. An equilibrium is achieved by performing a competitive waterfilling-based algorithm iteratively across all UTs in the network [11, 12]. Alternatively, the zero-forcing beamforming (ZFB) in [13–15] simplifies the non-convex structure of power allocations in multiuser MIMO-OFDM systems by eliminating interference via zero-forcing beamformers. This allows powers to be allocated to co-channel UTs by the waterfilling strategy in interference-free OFDM subchannels. However, the performance of ZFB is limited by the number of transmit antennas and the mutual orthogonality condition between the UT channel gains. Therefore, a user scheduling algorithm based on semi-orthogonal user selection in [16] is needed to select a subgroup of UTs that results in the lowest mutual interference.

In this paper, we propose a new suboptimal resource allocation algorithm for downlink multiuser MIMO-OFDM systems. The algorithm applies a successive convex approximation (SCA) technique in [17] to solve the optimisation problem of maximising weighted sum-rates subject to per-antenna and per-BS power constraints. In [17], the SCA technique is developed for solving a non-convex dynamic spectrum management in the digital

subscriber line (DSL) technology with cross-talk. The algorithm attempts to jointly optimise desired signal powers and interference powers through an iterative convex approximation procedure. The same technique has been extended to solve resource allocation problems for both single-cell MIMO-OFDM access (OFDMA) in [18] and multicell OFDMA in [19] wireless networks. This approach has been demonstrated to outperform the IWF algorithm [17].

The main contributions of this paper are summarised as follows:

• We establish an SCA-based optimisation framework for power and rate allocations of multiuser downlink MIMO-OFDM systems with CoMP with distributed transmit antennas to mitigate the effect of ICI. We design the precoding and postprocessing matrices based on the singular value decomposition (SVD) of each MIMO-OFDM subchannel to maximise spatial degrees of freedom of the MIMO channel. In doing so, we have applied the SCA algorithm for DSL in [17] to a new construction of MIMO-OFDM subchannels in our proposed system.

• We derive an iterative algorithm for solving the non-convex resource allocation problem efficiently. In doing so, we adopt the SCA algorithm in [17] to transform the non-convex problem into a convex one. This transformation allows us to develop an efficient algorithm to obtain a locally optimal solution via the dual Lagrange decomposition technique with the aid of a subgradient method [20]. We provide a convexity proof for the transformed problem and we show that the proposed algorithm can converge to a unique solution.

• We consider a practical aspect by imposing a power constraint on individual transmit antennas. This approach ensures that every transmit antenna will have the same average transmit power levels, regardless of the channel condition. In addition to this, the average transmit antenna power is limited in such a way that the resulting high peak power problem is indirectly controlled without exceeding the dynamic range of high-powered amplifiers (HPAs) for non-linear transmission effects. These effects, including signal clipping and saturation, are caused by the transmit signal exceeding the dynamic range of HPAs. This practical issue is often overlooked in resource allocation problems with a total transmit power constraint, where the majority of the total transmit power may be allocated to the antenna that has the best channel condition. This may cause the peak power issue to be even more problematic.

• We compare our proposed algorithm with two other suboptimal algorithms, namely IWF [12] and ZFB with semi-orthogonal user selection [16]. The comparisons between the algorithms are performed under both per-antenna and per-BS power constraints.

We envision the proposed algorithm to be more suited fixed-wireless applications in sparsely populated regions that require high data rate to UTs over very large network areas. An example is the provision of rural wireless broadband services to household modems where the channel gains are quasi-stationary [21]. Moreover, our proposed algorithm is also suitable for small cells with low user mobility.

This paper is structured as follows. The system model is introduced in Section 2. The formulation of weighted sum-rate maximisation problem is presented in Section 3. The concept of SCA-based algorithm is introduced in Section 4. Section 4 also includes proofs for the convexity of approximated optimisation problem transformed by the SCA-based algorithm and the convergence of the algorithm. Section 5 presents the numerical comparison between SCA, IWF and ZFB under both per-antenna and per-BS power constraints. Concluding remarks are presented in Section 6.

## 2 System model

We consider a multiuser MIMO-OFDM system with $N$ subchannels and CoMP transmission as shown in Fig. 1. The system consists of $M$ cooperating BSs, each equipped with $L_T$ transmit antennas. These
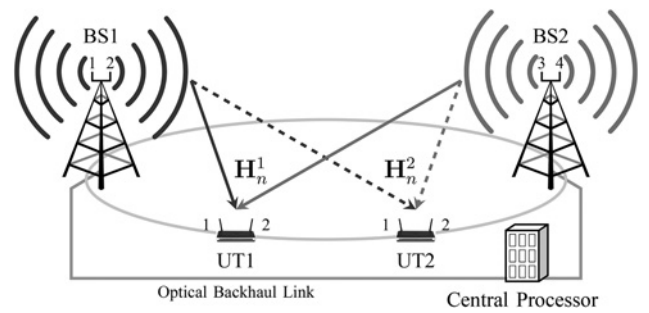


**Fig. 1** *Illustration of a MIMO-OFDM system with $M = 2$ CoMP BSs transmitting to $K = 2$ UTs and $L_T = L_R = 2$*

BSs employ CoMP with joint processing to simultaneously transmit to $K$ UTs, each equipped with $L_R$ receive antennas. We define $L = \min(ML_T, L_R)$ as the spatial degree of freedom of each MIMO-OFDM subchannel. We assume that perfect knowledge of the channel gains between all antennas and in each subchannel is known to both transmitters and receivers. The BSs are connected via high-speed optical backhaul links to a CP that allows the exchange of channel gains and user data. This permits a centralised implementation of our proposed power and rate allocation algorithm at the cooperating BSs.

The discrete-time received signal for the $k$th UT in the $n$th MIMO-OFDM subchannel, which is denoted as $\boldsymbol{y}_n^k \in \mathbb{C}^{L_R \times 1}$, after postprocessing is given by

$$\boldsymbol{y}_n^k = \boldsymbol{U}_n^{k^H} \boldsymbol{H}_n^k \boldsymbol{V}_n^k \sqrt{\boldsymbol{P}_{n,m}} \boldsymbol{x}_n^k + \boldsymbol{w}_n^k, \tag{1}$$

where $\boldsymbol{U}_n^{k^H} \in \mathbb{C}^{L_R \times L_R}$, $\boldsymbol{H}_n^k \in \mathbb{C}^{L_R \times ML_T}$ and $\boldsymbol{V}_n^k \in \mathbb{C}^{ML_T \times ML_T}$ are the postprocessing, complex channel gain and precoding matrices, respectively. The transmitted signals is denoted as $\boldsymbol{x}_n^k \in \mathbb{C}^{ML_T \times 1}$ and the complex Gaussian noise is denoted as $\boldsymbol{w}_n^k \in \mathbb{C}^{L_R \times 1}$ with variance $\sigma_n^2$. We define the diagonal matrix of transmitted powers in the $n$th subchannel from the $m$th transmit antenna as $\sqrt{\boldsymbol{P}_{n,m}} = \mathrm{diag}\left(\sqrt{P_{n,1}}, \ldots, \sqrt{P_{n,ML_T}}\right)$. The operator $(\cdot)^H$ represents the Hermitian transpose. In (1), the precoding and postprocessing matrices are obtained from the SVD of the channel matrix $\boldsymbol{H}_n^k$ which is given by

$$\boldsymbol{H}_n^k = \boldsymbol{U}_n^k \boldsymbol{\Lambda}_n^k \boldsymbol{V}_n^{k^H}, \tag{2}$$

where $\boldsymbol{\Lambda}_n^k$ is the $L \times L$ diagonal matrix with non-negative singular values of $\sqrt{\gamma_{n,l}^k}$, $l = 1, \ldots, L$ as the channel gain for the $(n, l)$th spatial-subchannel [22].

The aim of employing SVD is to decouple each MIMO-OFDM subchannel into $L$ independent parallel spatial-subchannels with the singular values squared as the subchannel gains. This decomposition, known as eigenbeamforming [23], is accomplished by applying the linear transformation $\boldsymbol{V}_n^k$ to the transmitted symbol vector and applying the linear transformation $\boldsymbol{U}_n^{k^H}$ to the received symbol vector. The resulting cascaded channel can be written as

$$\boldsymbol{U}_n^{k^H} \boldsymbol{H}_n^k \boldsymbol{V}_n^k = \boldsymbol{U}_n^{k^H} \boldsymbol{U}_n^k \boldsymbol{\Lambda}_n^k \boldsymbol{V}_n^{k^H} \boldsymbol{V}_n^k = \boldsymbol{\Lambda}_n^k. \tag{3}$$

As a result, an $N$-subchannel MIMO-OFDM system is decomposed to form a total of $N \times L$ spatial-subchannels. Assuming full knowledge of the channel gains, the overall system throughput can be optimised by implementing resource allocation algorithms across all the spatial-subchannels.

In formulating the optimisation problem, we distinguish between the following two domains: (i) 'antenna domain' and (ii) 'spatial domain'. The antenna domain consists of the signals and powers that are physically transmitted by the antennas. The spatial

domain, on the other hand, consists of the 'effective' powers and signals sent in the spatial-subchannels. We define the following terms:

$$\tilde{R}_{n,l}^{k} = \text{spatial rate in } (n, \ l)\text{th spatial} - \text{subchannel for UT } k$$

$$\tilde{P}_{n,l}^{k} = \text{spatial power in } (n, \ l)\text{th spatial} - \text{subchannel for UT } k$$

$$P_{n,m} = \text{transmit power in subchannel } n \text{ from antenna } m,$$

where a spatial-subchannel pair is denoted by subscript $(n, l)$ with $\sim$ and an antenna–subchannel pair is denoted by subscript $(n, m)$.

In the optimisation problem for the proposed power and rate allocation algorithm, we consider a continuous bit-loading scheme and express the achievable rate of the $k$th UT in the $(n, \ l)$th spatial-subchannel as

$$\tilde{R}_{n,l}^{k}\left(\widetilde{\boldsymbol{P}}_n\right) = \log_2\left[1 + \text{SINR}_{n,l}^{k}\left(\widetilde{\boldsymbol{P}}_n\right)\right], \quad (4)$$

where the signal-to-interference-plus-noise ratio (SINR) of the $k$th UT in the $(n, \ l)$th spatial-subchannel is defined as

$$\text{SINR}_{n,l}^{k}\left(\widetilde{\boldsymbol{P}}_n\right) = \frac{G_{n,l}^{k,k}\tilde{P}_{n,l}^{k}}{\sum_{j \neq k}^{K}(l, \ :)\widetilde{\boldsymbol{P}}_n^{j} + \sigma_{n,l}^{k2}},$$

$$\forall l = 1, \ \ldots, L. \quad (5)$$

The term $G_{n,l}^{k,k}$ is the $(n, \ l)$th spatial-subchannel gain obtained from the SVD of the corresponding channel matrix $\boldsymbol{H}_n^k$ and the interference channel gain $\boldsymbol{G}_n^{k,j}(l, :)$ is the $l$th row of the matrix $\boldsymbol{G}_n^{k,j}$ for the $n$th OFDM subchannel between the $k$th UT and the $j$th UT. We use the ':' notation to refer to each column or row in the corresponding matrix. For notational convenience, we write $\widetilde{\boldsymbol{P}}_n = [\widetilde{\boldsymbol{P}}_n^1 \ldots \widetilde{\boldsymbol{P}}_n^K]$ as the $L \times K$ spatial power matrix for the $n$th OFDM subchannel, where each $\widetilde{\boldsymbol{P}}_n^k = [\tilde{P}_{n,1}^k \ldots \tilde{P}_{n,L}^k]^{\text{T}}$ is the $L \times 1$ spatial power vector for the $k$th UT in the $n$th OFDM subchannel. The noise variance of the $k$th UT in the $(n, \ l)$th spatial-subchannel is expressed as $\sigma_{n,l}^{k2}$ and we assume the noise variances are constant and equal across all the spatial-subchannels. The interference channel gain $\boldsymbol{G}_n^{k,j}$ is defined as

$$\boldsymbol{G}_n^{k,j}(x, y) = \left|\boldsymbol{U}_n^{k\text{H}}(:, x)\boldsymbol{H}_n^k\boldsymbol{V}_n^j(:, y)\right|^2, \quad \forall x, y = 1, \ \ldots, L, \quad (6)$$

where the terms $\boldsymbol{U}_n^{k\text{H}}(:, x)$ and $\boldsymbol{V}_n^j(:, y)$ are the $x$th and $y$th columns of the matrices $\boldsymbol{U}_n^{k\text{H}}$ and $\boldsymbol{V}_n^j$, respectively. The physical interpretation of the SVD on the MIMO channel is particularly useful from the antenna perspective. For a given eigenvalue $\gamma_{n,l}^k$ of $\boldsymbol{H}_n^k\boldsymbol{H}_n^{k\text{H}}$, the precoding matrix $\boldsymbol{V}_n^k$ is the transmit beamforming weights on each antenna for transmitting signals in the corresponding spatial-subchannels. The conjugate match of the postprocessing matrix $\boldsymbol{U}_n^{k\text{H}}$ gives the receive power gain of $\gamma_{n,l}^k$. A mismatch between the precoding and postprocessing matrices in (6) results in a weighted sum of all interfering signals, which are defined as the interference function from the $j$th UT projecting onto the receiving direction of the $k$th UT. Our proposed resource allocation algorithm aims to provide an interference management such that the total sum-rate in (4) is maximised for given antenna power constraints.

## 3 Optimisation problem formulation

In this section, we formulate the MIMO-OFDM resource allocation problem as a rate adaptive (RA) problem. The RA problem aims to maximise the weighted sum-rate or the overall system throughput subject to a total transmit power constraint. In this paper, however,

we consider a practical scenario by replacing the total transmit power constraint with per-antenna power constraints. The per-antenna power constraint prevents unbalanced power allocation amongst all the transmit antennas. In the case of the total transmit power constraint, the majority of the power would be allocated to the BS and corresponding antennas with the most favourable channel conditions. This would cause some transmit antennas and their associated peak powers to be even higher compared to ones with per-antenna power constraints, and thereby require more expensive HPAs with a large dynamic range to transmit signals without non-linear transmission effects. The consideration of per-antenna power constraints limits the average transmit antenna powers which indirectly control the resulting peak power to a tolerable level.

We propose to compute the optimal power allocation that maximises the weighted sum-rate of a downlink multiuser MIMO-OFDM system subject to a set of individual antenna power constraints. The optimisation problem can be formulated as

$$\underset{\forall P_{n,m} \geq 0}{\text{maximise}} \quad \sum_{k=1}^{K} \sum_{n=1}^{N} \sum_{l=1}^{L} \omega_k \tilde{R}_{n,l}^{k}\left(\widetilde{\boldsymbol{P}}_n\right)$$

$$\text{subject to} \quad \sum_{n=1}^{N} P_{n,m} \leq P_{\max}^m, \quad \forall m = 1, \ \ldots, ML_{\text{T}}, \quad (7)$$

where $P_{\max}^m$ is the $m$th antenna power constraint and $\omega_k$ is the positive weight associated with the $k$th UT. These weights can be used to classify different quality of service constraints or to prioritise services based on various data throughput requirements or the premium paid by service subscribers.

To simplify the optimisation in (7), we establish a relationship between spatial average powers and antenna average powers in the following lemma. Provided the data symbols sent in each spatial-subchannel are uncorrelated (as is expected) with zero mean and normalised to unit variance, it can be shown by the following lemma.

*Lemma 1:* The relationship between antenna powers $\boldsymbol{P}_n^k$ and spatial powers $\widetilde{\boldsymbol{P}}_n^k$ is given by $\boldsymbol{P}_n^k = A_n^k\widetilde{\boldsymbol{P}}_n^k$, where $A_n^k(m, \ l) = \left|V_n^k(m, \ l)\right|^2$.

*Proof:* Let $\tilde{\boldsymbol{x}}_n^k$ be the uncorrelated data symbols sent in each spatial-subchannel that have zero mean and normalised to unit variance. Then $\tilde{\boldsymbol{x}}_n^k$ undergoes a linear transformation with the precoding matrix $\boldsymbol{V}_n^k$, which is given by $\boldsymbol{x}_n^k = \boldsymbol{V}_n^k\tilde{\boldsymbol{x}}_n^k$. The relationship between antenna average powers and spatial average powers can be derived as

$$\boldsymbol{P}_n^k = \text{Tr}\left\{\mathbb{E}\left[\boldsymbol{x}_n^k\boldsymbol{x}_n^{k\text{H}}\right]\right\}$$

$$= \left|\begin{bmatrix} v_{1,1}^k & \cdots & v_{1,ML_T}^k \\ \vdots & \ddots & \vdots \\ v_{ML_T,1}^k & \cdots & v_{ML_T,ML_T}^k \end{bmatrix}\right|^2 \mathbb{E}\left[\left|\tilde{\boldsymbol{x}}_n^k\right|^2\right]$$

$$= \left|\boldsymbol{V}_n^k\right|^2\widetilde{\boldsymbol{P}}_n^k, \quad (8)$$

where $\text{Tr}(\cdot)$ is denoted as the trace of a matrix and $|\cdot|^2$ is denoted as the squared magnitude operation. $\qquad \square$

In other words, $A_n^k$ is the 'power gain transformation' from spatial powers to antenna powers in the $n$th OFDM subchannel for the $k$th UT and is equal to the element-by-element squared magnitude of $\boldsymbol{V}_n^k$.

The optimisation problem in (7) presents a great challenge for obtaining the globally optimal solution. Rewriting the objective

function in (7) in the following expression:

$$
\begin{aligned}
\tilde{R}_{n,l}^{k}\left(\widetilde{\boldsymbol{P}}_{n}\right) &= \log_{2}\left[1 + \mathrm{SINR}_{n,l}^{k}\left(\widetilde{\boldsymbol{P}}_{n}\right)\right] \\
&= \log_{2}\left[1 + \frac{\mathrm{G}_{n,l}^{k,k}\tilde{P}_{n,l}^{k}}{\sum_{j\neq k}^{K}\boldsymbol{G}_{n}^{k,j}(l,\,:)\widetilde{\boldsymbol{P}}_{n}^{j} + \sigma_{n,l}^{k^{2}}}\right] \\
&= \log_{2}\left[\mathrm{G}_{n,l}^{k,k}\tilde{P}_{n,l}^{k} + \sum_{j\neq k}^{K}\boldsymbol{G}_{n}^{k,j}(l,\,:)\widetilde{\boldsymbol{P}}_{n}^{j} + \sigma_{n,l}^{k^{2}}\right] \\
&\quad - \log_{2}\left[\sum_{j\neq k}^{K}\boldsymbol{G}_{n}^{k,j}(l,\,:)\widetilde{\boldsymbol{P}}_{n}^{j} + \sigma_{n,l}^{k^{2}}\right].
\end{aligned} \tag{9}
$$

It can be seen that the expression in (9) is of the form of a difference of concave functions (DoCFs) in $\boldsymbol{P}_{n}$. Functions with a DoCF structure is difficult to solve as these functions are generally non-convex and NP-hard for obtaining globally optimal solutions [24].

## 4 Proposed SCA algorithm

In this section, we introduce the SCA-based algorithm in [17] to overcome the DoCF structure of the objective function in (9). The SCA-based algorithm converts a non-convex optimisation problem into a convex one by an iterative convex approximation technique. This approximation is based on the following lower bound:

$$
\log_{2}(1 + x) \geq \alpha \log_{2} x + \beta, \tag{10}
$$

where $\alpha$ and $\beta$ are the convex approximation constants, which dictate the accuracy of this lower bound approximation on the Pareto boundary of the achievable rate region. The approximated lower bound is tight at $x = \bar{x}$ when the approximation constants are chosen as

$$
\alpha = \frac{\bar{x}}{1 + \bar{x}} \tag{11a}
$$

$$
\beta = \log_{2}(1 + \bar{x}) - \frac{\bar{x}}{1 + \bar{x}}\log_{2}\bar{x}. \tag{11b}
$$

The lower bound in (10) is improved successively by updating $\alpha$ and $\beta$ according to (11a) and (11b), respectively, at each iteration based on the new value of $\bar{x}$. A locally optimal solution can be obtained as the lower bound converges to the achievable rate region.

Applying the lower bound in (10) to the objective function in (9) and converting the antenna powers to spatial powers using Lemma 1, the RA optimisation problem in (7) can be approximated by

$$
\underset{\forall \widetilde{\boldsymbol{P}}_{n}\succeq 0}{\text{maximise}} \quad \sum_{k=1}^{K}\sum_{n=1}^{N}\sum_{l=1}^{L}\omega_{k}\left\{\alpha_{n,l}^{k}\log_{2}\left[\mathrm{SINR}_{n,l}^{k}\left(\widetilde{\boldsymbol{P}}_{n}\right)\right] + \beta_{n,l}^{k}\right\}
$$

$$
\text{subject to} \quad \sum_{k=1}^{K}\sum_{n=1}^{N}A_{n}^{k}(m,\,:)\widetilde{\boldsymbol{P}}_{n}^{k} \leq P_{\max}^{m}, \quad \forall m = 1,\,\ldots,\,ML_{\mathrm{T}}, \tag{12}
$$

where the approximation constants for the $(n,\,l)$th spatial-subchannel are denoted as $\alpha_{n,l}^{k}$ and $\beta_{n,l}^{k}$. We note that the objective function in (12) is still non-convex due to the presence of the DoCF structure. To avoid the DoCF structure, we rewrite the objective function in

(12) using the substitution of $\widetilde{\boldsymbol{P}}_{n} = \mathrm{e}^{\widehat{\boldsymbol{P}}_{n}}$, which is given by

$$
\begin{aligned}
\tilde{R}_{n,l}^{k} &\geq \alpha_{n,l}^{k}\log_{2}\left[\mathrm{SINR}_{n,l}^{k}\left(\mathrm{e}^{\widehat{\boldsymbol{P}}_{n}}\right)\right] + \beta_{n,l}^{k} \\
&= \alpha_{n,l}^{k}\log_{2}\left[\frac{\mathrm{G}_{n,l}^{k,k}\mathrm{e}^{\hat{P}_{n,l}^{k}}}{\sum_{j\neq k}^{K}\boldsymbol{G}_{n}^{k,j}(l,\,:)e^{\widehat{\boldsymbol{P}}_{n}^{j}} + \sigma_{n,l}^{k^{2}}}\right] + \beta_{n,l}^{k} \\
&= \frac{\alpha_{n,l}^{k}}{\ln 2}\left\{\ln\mathrm{G}_{n,l}^{k,k} + \hat{P}_{n,l}^{k} - \ln\left[\sum_{j\neq k}^{K}\boldsymbol{G}_{n}^{k,j}(l,\,:)e^{\widehat{\boldsymbol{P}}_{n}^{j}} + \sigma_{n,l}^{k^{2}}\right]\right\} + \beta_{n,l}^{k}.
\end{aligned} \tag{13}
$$

The achievable rate function in (13) is now a convex function in $\widehat{\boldsymbol{P}}_{n}$. The convexity of the SCA transformation is formally presented in the following lemma.

*Lemma 2:* The achievable rate function in (13) is convexified by the transformation of $\widetilde{\boldsymbol{P}}_{n} = \mathrm{e}^{\widehat{\boldsymbol{P}}_{n}}$.

*Proof:* To show the achievable rate function in (13) is a convex function in $\widehat{\boldsymbol{P}}_{n}$, we need to show that the function

$$
f(\widehat{\boldsymbol{P}}_{n}) = \ln\left[\sum_{j\neq k}^{K}\boldsymbol{G}_{n}^{k,j}(l,\,:)\mathrm{e}^{\widehat{\boldsymbol{P}}_{n}^{j}} + \sigma_{n,l}^{k^{2}}\right] \tag{14}
$$

is a convex function since the first term in the parentheses in (13), $\ln\mathrm{G}_{n,l}^{k,k}$ is a positive constant and the second term $\hat{P}_{n,l}^{k}$ is an affine function with respect to $\widehat{\boldsymbol{P}}_{n}$. To show the function $f(\widehat{\boldsymbol{P}}_{n})$ is a convex function, we need to show that the Hessian of $f(\widehat{\boldsymbol{P}}_{n})$ is in fact a positive semi-definite matrix. The Hessian of $f(\widehat{\boldsymbol{P}}_{n})$ is given by Boyd and Vandenberghe [20]

$$
\nabla^{2}f(\widehat{\boldsymbol{P}}_{n}) = \frac{1}{Z^{2}}\left(Z\,\mathrm{diag}(\boldsymbol{z}) - \boldsymbol{z}\boldsymbol{z}^{\mathrm{T}}\right), \tag{15}
$$

where the term $\boldsymbol{z}$ is defined as

$$
\begin{aligned}
\boldsymbol{z} = (&\boldsymbol{G}_{n}^{k,1}(l,\,:)\mathrm{e}^{\widehat{\boldsymbol{P}}_{n}^{1}},\,\ldots,\,\boldsymbol{G}_{n}^{k,k-1}(l,\,:)\mathrm{e}^{\widehat{\boldsymbol{P}}_{n}^{k-1}}, \\
&\boldsymbol{G}_{n}^{k,k+1}(l,\,:)\mathrm{e}^{\widehat{\boldsymbol{P}}_{n}^{k+1}},\,\ldots,\,\boldsymbol{G}_{n}^{k,K}(l,\,:)\mathrm{e}^{\widehat{\boldsymbol{P}}_{n}^{K}})
\end{aligned} \tag{16}
$$

and $Z$ is defined as

$$
Z = \sum_{j=1}^{K-1}z_{j} + \sigma_{n,l}^{k^{2}}. \tag{17}
$$

For $\boldsymbol{y} \in \mathbb{R}^{K-1}$, we define $L = \boldsymbol{y}^{\mathrm{T}}\nabla^{2}f(\widehat{\boldsymbol{P}}_{n})\boldsymbol{y}$ and show that [20]

$$
\begin{aligned}
Z^{2}L &= \boldsymbol{y}^{\mathrm{T}}\left(Z\,\mathrm{diag}(\boldsymbol{z}) - \boldsymbol{z}\boldsymbol{z}^{\mathrm{T}}\right)\boldsymbol{y} \\
&= \left(\sum_{j=1}^{K-1}y_{j}^{2}z_{j}\right)\left(\sum_{j=1}^{K-1}z_{j} + \sigma_{n,l}^{k^{2}}\right) - \left(\sum_{j=1}^{K-1}y_{j}z_{j}\right)^{2} \\
&\geq 0.
\end{aligned} \tag{18}
$$

The Cauchy–Schwarz inequality holds since $\sigma_{n,l}^{k^{2}}$ is non-negative. Therefore, the Hessian $\nabla^{2}f(\widehat{\boldsymbol{P}}_{n})$ is a positive semi-definite matrix which implies that the achievable rate function in (13) is convex. $\square$

Next, we convert the convex approximation of the primal problem in (12) into an unconstrained dual optimisation problem and solve it by the Lagrange dual decomposition method. After obtaining the antenna power allocation, the corresponding rate allocations can be

evaluated using (4) and (5). By introducing a non-negative dual variable vector, $\boldsymbol{\lambda}$, where each element of the vector corresponds to an individual per-antenna power constraint in (7), the Lagrangian of the primal problem in (12) is defined as

$$\mathcal{L}_{\mathrm{RA}}\left\{\widehat{\boldsymbol{P}}_n,\ \boldsymbol{\lambda}\right\} = \sum_{k=1}^{K}\sum_{n=1}^{N}\sum_{l=1}^{L}\omega_k$$

$$\times\left\{\frac{\alpha_{n,l}^k}{\ln 2}\left[\ln \mathrm{G}_{n,l}^{k,k} + \hat{P}_{n,l}^k - \ln\left(\sum_{j\neq k}^{K}\boldsymbol{G}_n^{k,j}(l,\ :)\mathrm{e}^{\widehat{\boldsymbol{P}_n^j}} + \sigma_{n,l}^{k^2}\right)\right] + \beta_{n,l}^k\right\}$$

$$-\sum_{m=1}^{ML_{\mathrm{T}}}\lambda_m\left[\sum_{k=1}^{K}\sum_{n=1}^{N}\boldsymbol{A}_n^k(m,\ :)\mathrm{e}^{\widehat{\boldsymbol{P}_n^k}} - P_{\max}^m\right], \qquad (19)$$

where $\boldsymbol{\lambda} = \left[\lambda_1 \ldots \lambda_{ML_{\mathrm{T}}}\right]$ is the $1 \times ML_{\mathrm{T}}$ vector of Lagrange multipliers associated with the transmit antennas. The Lagrange dual objective function is then written as

$$g_{\mathrm{RA}}(\boldsymbol{\lambda}) = \min_{\widehat{\boldsymbol{P}}_n \succeq 0}\mathcal{L}_{\mathrm{RA}}\left\{\widehat{\boldsymbol{P}}_n,\ \boldsymbol{\lambda}\right\} \qquad (20)$$

and the Lagrange dual optimisation problem and the corresponding dual optimal solution $D_{\mathrm{RA}}^*$ is expressed as

$$D_{\mathrm{RA}}^* = \underset{\boldsymbol{\lambda} \succeq 0}{\mathrm{maximise}}\, g(\boldsymbol{\lambda}). \qquad (21)$$

Since the approximated primal problem is convex and the feasible set consists of a non-empty interior, which satisfies the Slater's condition [20], the duality gap between the optimal primal value $P_{\mathrm{RA}}^*$ and the optimal dual value $D_{\mathrm{RA}}^*$ becomes zero, given by

$$P_{\mathrm{RA}}^* = D_{\mathrm{RA}}^*. \qquad (22)$$

Consider the $g_{\mathrm{RA}}(\boldsymbol{\lambda})$ in (21) for a given $\boldsymbol{\lambda}$, we note that it can be simplified into $KN$ independent optimisation problems as

$$g_{\mathrm{RA}}(\boldsymbol{\lambda}) = \sum_{k=1}^{K}\sum_{n=1}^{N}\bar{g}_n^k(\boldsymbol{\lambda}) - \sum_{m=1}^{ML_{\mathrm{T}}}\lambda_m P_{\max}^m, \qquad (23)$$

where the term $\bar{g}_n^k(\boldsymbol{\lambda})$ is given by

$$\bar{g}_n^k(\boldsymbol{\lambda}) = \min_{\forall\widehat{\boldsymbol{P}}_n^k \succeq 0}\sum_{l=1}^{L}\frac{\omega_k\alpha_{n,l}^k}{\ln 2}$$

$$\times\left\{\ln \mathrm{G}_{n,l}^{k,k} + \hat{P}_{n,l}^k - \ln\left[\sum_{j\neq k}^{K}\boldsymbol{G}_n^{k,j}(l,\ :)\mathrm{e}^{\widehat{\boldsymbol{P}_n^j}} + \sigma_{n,l}^{k^2}\right]\right\} + \beta_{n,l}^k$$

$$-\sum_{m=1}^{ML_{\mathrm{T}}}\lambda_m\boldsymbol{A}_n^k(m,\ :)\mathrm{e}^{\widehat{\boldsymbol{P}_n^k}}. \qquad (24)$$

This result indicates that the dual problem can be solved by optimising $N$ independent dual subproblems for all $K$ UTs. As a result, the overall implementation cost can be reduced significantly if the same procedure is executed repeatedly for each subproblem, or alternatively, $K$ parallel processors can be adopted for solving $N$ dual subproblems simultaneously to improve the convergence time of the algorithm.

We solve the dual maximisation problem in (20) by finding the stationary point of the Lagrangian in (19) with respect to $\widehat{\boldsymbol{P}}_n$, with a fixed $\boldsymbol{\lambda}$

$$\frac{\partial}{\partial\widehat{\boldsymbol{P}}_n}\mathcal{L}_{\mathrm{RA}}\left\{\widehat{\boldsymbol{P}}_n,\ \boldsymbol{\lambda}\right\} = \omega_k\alpha_{n,l}^k$$

$$-\,\mathrm{e}^{\widehat{\boldsymbol{P}_n^k}}\left[c\boldsymbol{\lambda}\boldsymbol{A}_n^k(:,\ l) + \frac{\sum_{j\neq k}\boldsymbol{G}_n^{j,k}(l,\ :)\boldsymbol{\alpha}_n^j\omega_j}{\sum_{j\neq k}\boldsymbol{G}_n^{k,j}(l,\ :)\mathrm{e}^{\widehat{\boldsymbol{P}_n^j}} + \sigma_{n,l}^{k^2}}\right] = 0, \qquad (25)$$

where $c = \ln 2$. By substituting $\widehat{\boldsymbol{P}}_n = \ln \widetilde{\boldsymbol{P}}_n$ into (25) and rearranging the terms, we get

$$\tilde{P}_{n,l}^k = \frac{\omega_k\alpha_{n,l}^k}{c\boldsymbol{\lambda}\boldsymbol{A}_n^k(:,\ l) + \sum_{j\neq k}\boldsymbol{G}_n^{j,k}(l,\ :)\boldsymbol{\alpha}_n^j\omega_j\dfrac{\mathrm{SINR}_{n,l}^j\left(\widetilde{\boldsymbol{P}}_n\right)}{\mathrm{G}_{n,l}^{j,j}\tilde{P}_{n,l}^j}}, \qquad (26)$$

where $\boldsymbol{\alpha}_n^j = [\alpha_{n,1}^j \ldots \alpha_{n,L}^j]^{\mathrm{T}}$ is the $L \times 1$ convex approximation constant vector for the $n$th OFDM subchannel of the $j$th UT. To prove that the solution to the RA problem in (7) is unique, we show in Lemma 3 that (26) satisfies Yates' definition of a standard interference function given below.

*Definition 1:* An interference function $\mathcal{I}(\boldsymbol{p})$ is *standard* if for all $\boldsymbol{p} \succeq 0$ the following properties are satisfied:

- Positivity: $\mathcal{I}(\boldsymbol{p}) > 0$.
- Monotonicity: If $\boldsymbol{p} \succeq \boldsymbol{p}'$, then $\mathcal{I}(\boldsymbol{p}) \geq \mathcal{I}(\boldsymbol{p}')$.
- Scalability: For all $\theta > 1$, $\theta\mathcal{I}(\boldsymbol{p}) > \mathcal{I}(\theta\boldsymbol{p})$.

*Lemma 3:* The power allocation strategy in (26) is a standard interference function.

*Proof:* We rewrite the power allocation in (26)

$$\mathcal{I}_{n,l}^k(\widetilde{\boldsymbol{P}}) \triangleq \frac{\omega_k\alpha_{n,l}^k}{c\boldsymbol{\lambda}\boldsymbol{A}_n^k(:,\ l) + \sum_{j\neq k}\dfrac{\boldsymbol{G}_n^{j,k}(l,\ :)\boldsymbol{\alpha}_n^j\omega_j}{\boldsymbol{G}_n^{k,j}(l,\ :)\widetilde{\boldsymbol{P}}_n^j + \sigma_{n,l}^{k^2}}}. \qquad (27)$$

We apply Definition 1 to (27) to show that the power allocation is unique and it can converge to a solution.

- Positivity: This follows from the fact that each term in $\mathcal{I}_{n,l}^k(\widetilde{\boldsymbol{P}})$ in (27) is non-negative.
- Montonicity: Suppose $\widetilde{\boldsymbol{P}} \geq \widetilde{\boldsymbol{P}}'$, the monotonicity property follows from

$$\mathcal{I}_{n,l}^k(\widetilde{\boldsymbol{P}}) = \frac{\omega_k\alpha_{n,l}^k}{c\boldsymbol{\lambda}\boldsymbol{A}_n^k(:,\ l) + \sum_{j\neq k}\dfrac{\boldsymbol{G}_n^{j,k}(l,\ :)\boldsymbol{\alpha}_n^j\omega_j}{\boldsymbol{G}_n^{k,j}(l,\ :)\widetilde{\boldsymbol{P}}_n^j + \sigma_{n,l}^{k^2}}}$$

$$\geq \frac{\omega_k\alpha_{n,l}^k}{c\boldsymbol{\lambda}\boldsymbol{A}_n^k(:,\ l) + \sum_{j\neq k}\dfrac{\boldsymbol{G}_n^{j,k}(l,\ :)\boldsymbol{\alpha}_n^j\omega_j}{\boldsymbol{G}_n^{k,j}(l,\ :)\widetilde{\boldsymbol{P}}_n^{j'} + \sigma_{n,l}^{k^2}}} = \mathcal{I}_{n,l}^k(\widetilde{\boldsymbol{P}}') \qquad (28)$$

- Scalability: Suppose $\widetilde{\boldsymbol{P}} = \theta \widetilde{\boldsymbol{P}}'$ for $\theta > 1$, the scalability property follows from

$$\theta \mathcal{I}_{n,l}^{k}(\widetilde{\boldsymbol{P}}) = \frac{\omega_k \alpha_{n,l}^{k}}{\dfrac{1}{\theta} c \boldsymbol{\lambda} \boldsymbol{A}_n^k(:,\ l) + \dfrac{1}{\theta} \sum_{j \neq k} \dfrac{\boldsymbol{G}_n^{j,k}(l,\ :) \boldsymbol{\alpha}_n^j \omega_j}{\boldsymbol{G}_n^{k,j}(l,\ :) \widetilde{\boldsymbol{P}}_n^j + \sigma_{n,l}^{k2}}}$$

$$> \frac{\omega_k \alpha_{n,l}^{k}}{c \boldsymbol{\lambda} \boldsymbol{A}_n^k(:,\ l) + \sum_{j \neq k} \dfrac{\boldsymbol{G}_n^{j,k}(l,\ :) \boldsymbol{\alpha}_n^j \omega_j}{\boldsymbol{G}_n^{k,j}(l,\ :) \theta \widetilde{\boldsymbol{P}}_n^{j\,'} + \sigma_{n,l}^{k2}}} = \mathcal{I}_{n,l}^{k}(\theta \widetilde{\boldsymbol{P}}')$$

(29)

$\square$

The term $\boldsymbol{G}_n^{k,j}(l,\ :)$ in (26) quantifies the mutual interference between the $k$th UT on all other UTs in the network on a spatial-subchannel-by-spatial-subchannel basis. The power allocation strategy in (26) allocates power to co-channel UTs that have the least amount of mutual interference between them. In the case of high mutual interference between UTs, the strategy in (26) allows no sharing of the subchannel and allocate power only to the UT that has the largest channel gain. We note that there is no explicit processing steps for the subchannels allocation, but that it is performed implicitly based on the value of $\boldsymbol{G}_n^{k,j}(l,\ :)$.

By combining the result in (26) and the dual decomposition method in (24), we propose an iterative SCA algorithm to solve the RA problem in (7). We begin the algorithm by initialising $\boldsymbol{\alpha} = 1$ and $\boldsymbol{\beta} = 0$ based on a high-signal-to-noise ratio approximation [17]. (With the initialisation of $\boldsymbol{\alpha} = 1$ and $\boldsymbol{\beta} = 0$, we assume that we have no previous knowledge of the initial power allocation for all UTs across all OFDM subchannels (i.e. $\tilde{P}_{n,l}^{k} = 0,\ \forall k,\ n,\ l$). Therefore, there is no interference at the initial step of the proposed algorithm, which results in a high SINR.) At each iteration, the lower bound is tightened by updating the $\boldsymbol{\alpha}$ and $\boldsymbol{\beta}$, using on (11a) and (11b), respectively, based on the new SINR values

$$\bar{x}_n^{k[s+1]} = \mathbf{SINR}_n^k \left( \widetilde{\boldsymbol{P}}_n^{\ [s]} \right), \tag{30}$$

where $s$ is the number of iterations. To obtain the optimal solution from the dual domain, we employ a subgradient method in which the Lagrange multipliers are updated toward satisfying the per-antenna power constraint with equality and is given by

$$\lambda_m^{[s+1]} = \left\{ \lambda_m^{[s]} + \nu \left[ \sum_{k=1}^{K} \sum_{n=1}^{N} \boldsymbol{A}_n^k(m,\ :) \widetilde{\boldsymbol{P}}_n^{k[s+1]} - P_{\max}^m \right] \right\}^+, \tag{31}$$

where $\{\cdot\}^+ = \max(0,\ \cdot)$ and $\nu$ is a fixed step size. The updated Lagrange multipliers are then substituted into (26) to obtain new power allocations.

**Algorithm 1**

1: Initialise $s = 1$, $\boldsymbol{\alpha}_n^{k[1]} = 1$, $\boldsymbol{\beta}_n^{k[1]} = 0$, $\tilde{\mathbf{P}}^{[1]} = 0$, $\tilde{\mathbf{R}}^{[1]} = 0$ and $\boldsymbol{\lambda}^{[1]} = 1$

2: **while** $\left| P_{RA}^{[s]} - g_{RA}(\boldsymbol{\lambda}^{[s]}) \right| \geq$ desired accuracy $\epsilon$ **do**

3:     Evaluate $\tilde{P}_{n,l}^{k\ [s+1]}$ using (26) for a given $\boldsymbol{\lambda}^{[s]}$

4:     Evaluate $\tilde{R}_{n,l}^{k\ [s+1]}$ using (4) based on $\tilde{P}_{n,l}^{k\ [s+1]}$

5:     Update $\boldsymbol{\alpha}_n^{k[s+1]}$ and $\boldsymbol{\beta}_n^{k[s+1]}$ using (11a) and (11b), respectively, at $\bar{x}_n^k = \mathbf{SINR}_n^k \left( \tilde{\mathbf{P}}_n^{[s+1]} \right)$

6:     Compute the primal objective $P_{RA}^{[s]}$ in (7)

7:     Compute the dual objective $g_{RA}\left( \boldsymbol{\lambda}^{[s]} \right)$ (20)

8:     Update each element of $\boldsymbol{\lambda}^{[s+1]}$ using (31)

9:     Increment $s$

10: **end while**

**Fig. 2** *SCA algorithm*

Solving this optimisation problem consists of two main steps that are applied iteratively:

- *Step 1*: For a given Lagrange multiplier vector $\boldsymbol{\lambda}$, find the minimum Lagrangian cost function by performing power allocations using in (26). This results in the optimal solution for a set of antenna power constraints, but not necessarily those specified in (12).
- *Step 2*: Update $\boldsymbol{\lambda}$ based on the subgradient of the first step results using (31) in order to increase $g_{RA}(\boldsymbol{\lambda})$ and eventually achieve (21). Go to step 1.

The iterative procedure terminates when a stopping criteria is satisfied (i.e. the duality gap between the primal and dual objective functions approaches zero). The SCA algorithm is summarised in Fig 2.

## 5 Simulation results and discussion

Numerical simulation results are presented in this section based on a two-cell fixed-wireless MIMO-OFDM downlink system with $N = 32$ OFDM subchannels as shown in Fig. 3. Each BS is equipped with $L_T = 2$ antennas with a per-antenna power constraint of 20 W. The BSs are assumed to be connected to a CP by a high-speed optical backhaul to execute the proposed algorithm. We set $K = 5$ UTs in the simulation and each is equipped with $L_R = 2$ antennas. The UTs are randomly distributed within a circular radius of 100 m located between the cells to model a cell-edge environment. The MIMO channel gains for each OFDM subchannel are modelled as zero-mean circularly symmetric complex Gaussian random variables with a unit variance, that is, $\boldsymbol{H}_n \sim \mathcal{CN}(0,\ \boldsymbol{I})$. The path loss is modelled by the COST-231 Hata empirical model to simulate a typical deployment in rural (flat) environments, which is given by Goldsmith [22]

$$\begin{aligned} L_d = {}&46.3 + 33.9 \log_{10} f - 13.82 \log_{10} h_t - a(h_r) \\ &+ (44.9 - 6.55 \log_{10} h_t) \log_{10} d + C_m, \end{aligned} \tag{32}$$

where $f$ is the carrier frequency in megahertz, $d$ is the distance between BS and UT antennas in kilometres and $h_t$ is the height of the BS above ground level in metres. The parameter $C_m$ is defined as 0 dB for suburban or rural environments and 3 dB for metropolitan environments. The parameter $a(h_r)$ is defined for rural environments as [22]

$$a(h_r) = (1.1 \log_{10} f - 0.7) h_r - (1.56 \log_{10} f - 0.8), \tag{33}$$

where $h_r$ is the height of the UT above ground level in metres. The simulation parameters from [22, 25, 26] are given in Table 1.
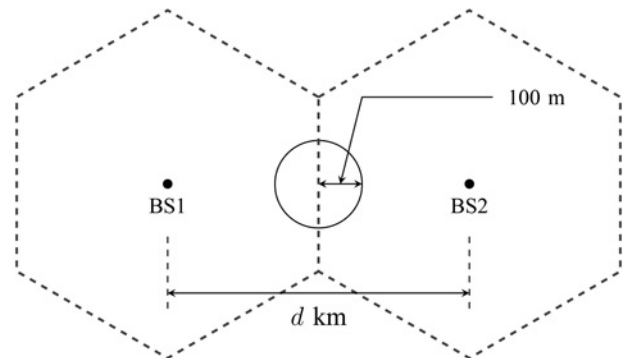


**Fig. 3** *Two-cell MIMO-OFDM network with downlink CoMP and UTs located at the cell-edge. We vary the distance between BSs to model different CNRs*

**Table 1** COST-231 path-loss model parameters [22, 25, 26]

| Simulation parameters | |
|---|---|
| bandwidth, MHz | 10 |
| carrier frequency, GHz | 2 |
| BS height, m | 30 |
| maximum Tx power, dBm | 46 |
| RF feeder cable/connector loss, dB | 2 |
| antenna gain, dBi | 18 |
| receiver height, m | 5 |
| antenna gain, dBi | 8 |
| noise figure, dB | 7 |
| thermal noise, dBm/Hz | −174 |
| receiver noise floor, dBm | −97 |
| slow fading margin, dB | 8 |



**Fig. 5** *Sum-rate performance comparison between SCA, IWF and ZFB in medium-interference environments with per-antenna power constraints and d = 20 km*

In the simulation results, we vary the distance between the cooperating BSs, which is denoted as $d$, ranging from 5 to 40 km for a typical LTE macrocell deployment [26]. On the basis of these distances, we can evaluate the received channel-to-noise ratio (CNR) on the $(n, l)$th spatial-subchannel for the $k$th UT as [27]

$$\mathrm{CNR}_{n,l}^{k} = \frac{\Lambda_{n,l}^{k^{2}}}{\sigma_{n,l}^{k^{2}}}, \tag{34}$$

where $\Lambda_{n,l}^{k}$ is the effective channel gain after precoding and postprocessing. The noise power is assumed to be equal across all OFDM subchannels. We average the simulation results over a total of 16,000 channel realisations, which is obtained from 100 simulation iterations for each UT subchannel. For simplicity, we assume the positive weight $\omega_{k} = 1$ in (7) across all UTs.
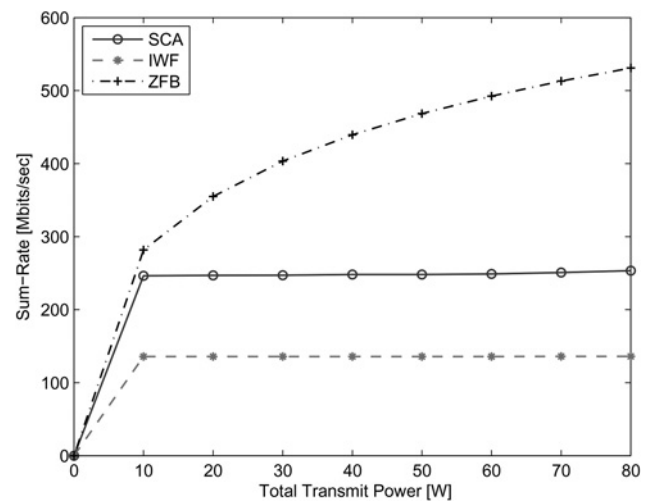
Fig. 4 compares the sum-rate performance between the proposed SCA, IWF in [12] and ZFB with semi-orthogonal user selection scheme in [16]. The BS-to-BS separation distance is $d = 40$ km. The resulting average received CNR = −4.54 dB models a low-interference environment where the interference power is insignificant compared with the noise power. We see that both SCA and IWF provide similar sum-rate performances of ∼23 Mbits/s for a total transmit power of 80 W. ZFB achieves the lowest sum-rate of 13 Mbits/s for 80 W between the cooperating BSs. The sum-rate performance of ZFB is affected by the reduction in effective channel gains for scheduled UTs as a result of performing ZFB on the channel gains of the scheduled UTs.

Fig. 5 demonstrates the sum-rate performance for a BS-to-BS separation of $d = 20$ km. The resulting average received CNR = −0.11 dB indicates a medium interference environment where the
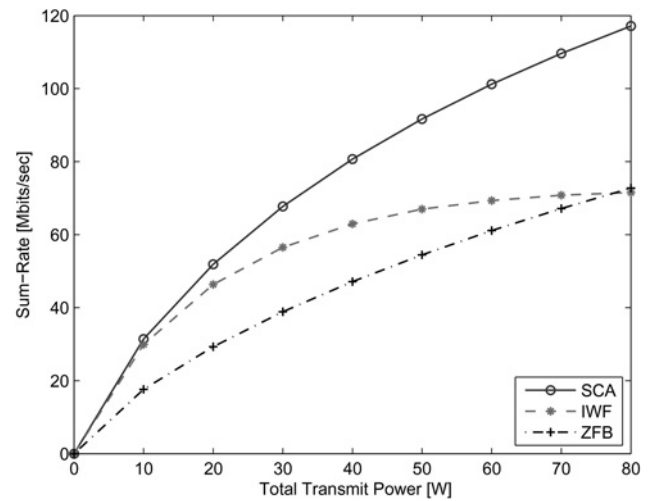
noise power is comparable with the interference power. In this scenario, the proposed SCA algorithm achieves the highest sum-rate performance compared with IWF and ZFB. For a total transmit power of 80 W between BSs, we note that SCA provides a better interference management compared with IWF which is limited by the interference at a sum-rate of 70 Mbits/s in the high transmit power regime. Despite cancelling interference for scheduled UTs, ZFB offers a slightly better sum-rate performance of 72 Mbits/s compared with 70 Mbits/s for IWF. The sum-rate performance of ZFB is affected by the reduction in effective channel gains for scheduled UTs as a result of performing ZFB on the channel gains of the scheduled UTs.

Fig. 6 shows the sum-rate performance comparison for a BS-to-BS separation distance of $d = 5$ km. This results in an average received CNR = 21.12 dB to model a high interference environment where the noise power is insignificant compared with the interference power. The plot shows that both SCA and IWF are limited by the severity of the interference power. However, we see that SCA still provides a better interference management with a sum-rate improvement of 110 Mbits/s compared with IWF for a total transmit power of 80 W. As expected, ZFB achieves the best



**Fig. 4** *Sum-rate performance comparison between SCA, IWF and ZFB in low-interference environments with per-antenna power constraints and d = 40 km*



**Fig. 6** *Sum-rate performance comparison between SCA, IWF and ZFB in high-interference environments with per-antenna power constraints and d = 5 km*
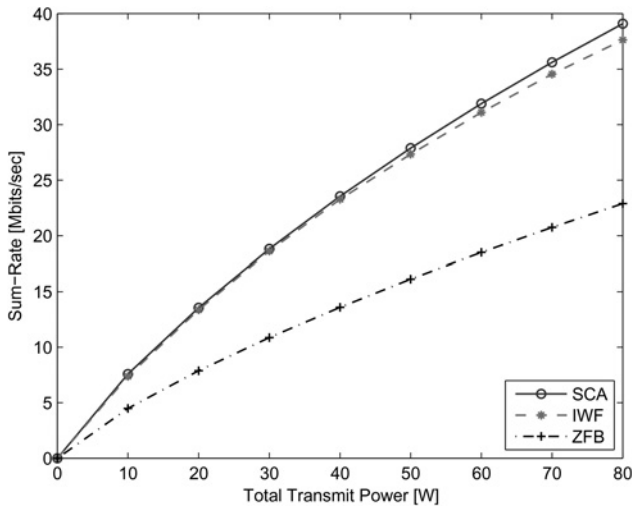
**Fig. 7** *Sum-rate performance comparison between SCA, IWF and ZFB in low interference environments with per-BS power constraints and d = 40 km*

performance of 520 Mbits/s for a total transmit power of 80 W as it provides interference-free subchannels for the scheduled UTs.

Next, we consider the same system and simulation parameters with per-BS power constraints instead of per-antenna power constraints. As such we apply a power constraint of $L_T \times P_{max}^m$, $\forall m = 1, \ldots, M$ on individual BSs. This results in a simpler optimisation problem as the Lagrange search space reduces to one dimension per BS (i.e. $\lambda^m = \lambda_1^m = \ldots = \lambda_{L_T}^m$, $\forall m = 1, \ldots, M$), which results in the following optimisation problem

$$
\begin{aligned}
&\underset{\forall \boldsymbol{P}_n \succeq 0}{\text{maximise}} && \sum_{k=1}^{K} \sum_{n=1}^{N} \sum_{l=1}^{L} \omega_k \left\{ \alpha_{n,l}^k \log_2 \left[ \text{SINR}_{n,l}^k \left( \widetilde{\boldsymbol{P}}_n \right) \right] + \beta_{n,l}^k \right\} \\
&\text{subject to} && \sum_{t=1}^{L_T} \sum_{k=1}^{K} \sum_{n=1}^{N} A_n^k(t, :) \widetilde{\boldsymbol{P}}_n^k \le P_{max}^m, \quad \forall m = 1, \ldots, M,
\end{aligned}
\tag{35}
$$

where $P_{max}^m$ is the individual transmit power constraint on each BS. The Lagrange multipliers associated with each BS is updated by a
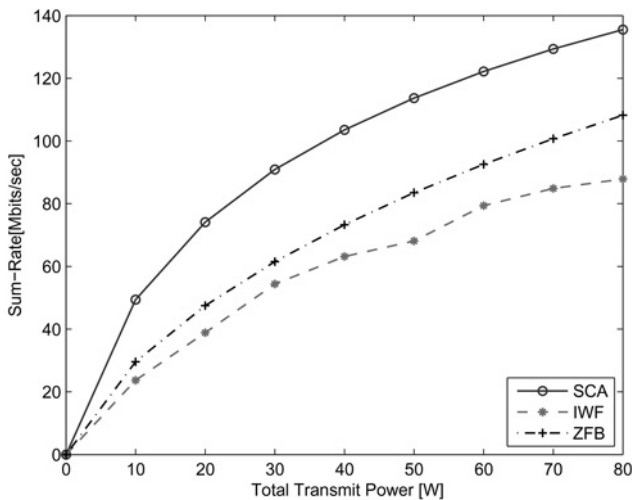


**Fig. 8** *Sum-rate performance comparison between SCA, IWF and ZFB in medium-interference environments with per-BS power constraints and d = 20 km*
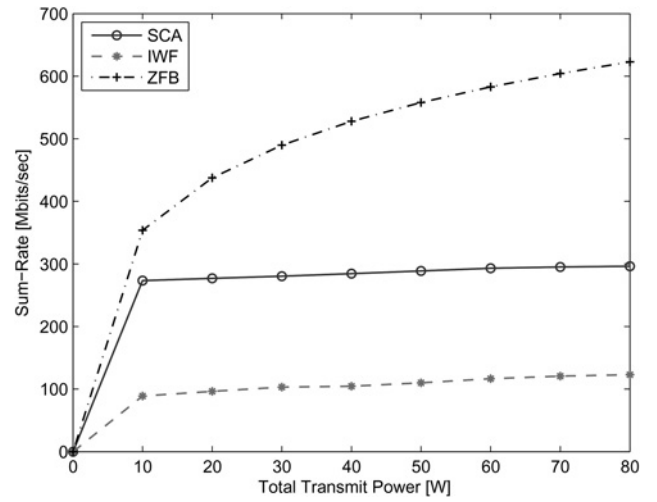


**Fig. 9** *Sum-rate performance comparison between SCA, IWF and ZFB in high interference environments with per-BS power constraints and d = 5 km*

subgradient method which is given by

$$
\lambda_m^{[s+1]} = \left\{ \lambda_m^{[s]} + \nu \left[ \sum_{t=1}^{L_T} \sum_{k=1}^{K} \sum_{n=1}^{N} A_n^k(t, :) \widetilde{\boldsymbol{P}}_n^{k[s+1]} - P_{max}^m \right] \right\}^+. \tag{36}
$$

Fig. 7 shows the sum-rate performance comparison between SCA, IWF and ZFB with $d = 40$ km in a low interference environment. We see a similar performance trend compared with the corresponding results with per-antenna power constraints in Fig. 3. The sum-rate performance with per-BS constraints results in an increase of ~15 Mbits/s for both SCA and IWF, whereas ZFB provides an increase of 10 Mbits/s with a 80 W of total transmit power between BSs.

Fig. 8 compares the sum-rate performance between SCA, IWF and ZFB in a medium interference environment with $d = 20$ km. ZFB outperforms IWF by ~30 Mbits/s, whereas SCA remains as the highest sum-rate performer with 138 Mbits/s with a total transmit power of 80 W.

Fig. 9 demonstrates the sum-rate performance comparison between SCA, IWF and ZFB in a high-interference environment with $d = 5$ km. Owing to severity of the interference, both SCA and IWF can only achieve 280 and 120 Mbits/sec, respectively, whereas ZFB provides 620 Mbits/s. We note that IWF still achieves the lowest sum-rate performance for a total transmit power of 80 W compared with SCA and ZFB under both per-antenna and per-BS power constraint scenarios.

Table 2 summarises the resulting individual antenna transmit powers for SCA, IWF and ZFB in various interference environments with per-BS power constraints. These individual

**Table 2** Resulting antenna transmit powers with per-BS power constraints in various interference environments

| | | BS1, dBm | | BS2, dBm | |
|---|---|---|---|---|---|
| | | Antenna number | | Antenna number | |
| | | #1 | #2 | #1 | #2 |
| high $d = 5$ km | SCA | 42.99 | 43.031 | 43.03 | 42.991 |
| | IWF | 42.992 | 43.029 | 43.018 | 43.003 |
| | ZFB | 42.999 | 43.022 | 43.012 | 43.009 |
| medium $d = 20$ km | SCA | 42.977 | 43.044 | 43.001 | 43.02 |
| | IWF | 42.911 | 43.108 | 43.146 | 42.871 |
| | ZFB | 43.014 | 43.007 | 42.975 | 43.046 |
| low $d = 40$ km | SCA | 42.979 | 43.042 | 42.982 | 43.039 |
| | IWF | 42.827 | 43.187 | 42.56 | 43.419 |
| | ZFB | 43.07 | 42.95 | 42.94 | 43.08 |

antenna transmit powers are expressed in decibels and figures in boldface represent the antenna transmit power that exceeds the per-antenna power constraint of $P_{max} = 20$ W or 43.01 dBm. The excess power in one of the transmit antennas in each BS would result in even a higher resulting peak power compared with the per-antenna power constraint scenarios. As a result, expensive HPAs with a large dynamic range maybe required in order to mitigate the effect of non-linear transmission caused by the exceeding peak powers.

## 6 Conclusion

We have introduced an optimisation approach for a downlink wireless multiuser MIMO-OFDM system with cooperating BSs. The approach utilised the SCA technique for maximising a sum-rate optimisation problem subject to per-antenna power constraints. The individual antenna power constraint offers the advantage of helping to constrain the peak power on each antenna (i.e. lower average powers result in lower peak powers) caused by the inherent problem of the high peak power in MIMO-OFDM systems.

Our numerical results demonstrate that SCA outperforms two common approaches: IWF and ZFB in low- and medium-interference environments. Despite the nulling of interference, the performance of ZFB is limited by the number of transmit antennas and the mutual orthogonality of the channel condition between serving UTs, which result in a much lower sum-rate performance than the SCA and IWF in low-interference environments. In high interference environments, ZFB outperforms SCA and IWF as these two algorithms are limited by the interference. The performance difference between the SCA and IWF depends on the interference between co-channel UTs. In general, the higher interference between UTs, the larger difference in sum-rate performances of these two algorithms. The approach of per-BS power constraints simplifies the optimisation problem to a one-dimensional Lagrange search space in each BS. Moreover, this approach results in higher sum-rate performances for SCA, IWF and ZFB compared with the more complicated per-antenna power constraints scenario. However, the practical issues of resulting high peak powers and unbalanced powers in transmit antennas need to be considered when designing and implementing the system using the per-BS power constraints.

A much more complicated problem would be the joint design of the spatial precoding and postprocessing matrices along with our approach. While this problem tends to be intractable, our approach could be applied on top of a coordinated beamforming method across all cooperating BSs.

We note that we have examined the performance of SCA based on the assumption of perfect knowledge of the channels. An interesting extension to this paper is to consider the impact of channel estimation errors in the proposed algorithm. It is expected that the use of estimated channels will result in a loss of diversity at the receiver as the SVD of the channel cannot effectively eliminate interference between co-channel users.

## 7 References

1 Ghosh, A., Ratasuk, R., Mondal, B., Mangalvedhe, N., Thomas, T.: 'LTE-advanced: next-generation wireless broadband technology', *IEEE Wirel. Commun.*, 2010, **17**, (3), pp. 10–22

2 Zhang, W., Xia, X.-G., Letaief, K.B.: 'Space-time/frequency coding for MIMO-OFDM in next generation broadband wireless systems', *IEEE Wirel. Commun.*, 2007, **14**, (3), pp. 32–43

3 Sampath, H., Talwar, S., Tellado, J., Erceg, V., Paulraj, A.: 'A fourth-generation MIMO-OFDM broadband wireless system: design, performance, and field trial results', *IEEE Commun. Mag.*, 2002, **40**, (9), pp. 143–149

4 Rey, F., Lamarca, M., Vazquez, G.: 'Robust power allocation for MIMO OFDM systems with imperfect CSI', *IEEE Trans. Signal Process.*, 2005, **3**, (3), pp. 1070–1085

5 Zhang, Y.J., Letaief, K.B.: 'An efficient resource-allocation scheme for spatial multiuser access in MIMO-OFDM systems', *IEEE Trans. Commun.*, 2005, **53**, (1), pp. 107–116

6 Björnson, E., Zakhour, R., Gesbert, D., Ottersten, B.: 'Cooperative multicell precoding: rate region characterization and distributed strategies with instantaneous and statistical CSI', *IEEE Trans. Signal Process.*, 2010, **58**, (8), pp. 4298–4310

7 Sawahashi, M., Kishiyama, Y., Morimoto, A., Nishikawa, D., Tanno, M.: 'Coordinated multipoint transmission/reception techniques for LTE-advanced', *IEEE Wirel. Commun. Mag.*, 2010, **17**, (3), pp. 26–34

8 Lee, D., Seo, H., Clerckx, B., Hardouin, E., Mazzarese, D., Sayana, S.N.K.: 'Coordinated multiple transmission and reception in LTE-advanced: deployment scenarios and operational challenges', *IEEE Commun. Mag.*, 2012, **50**, (2), pp. 148–155

9 Irmer, R., Droste, H., Marsch, P., *et al.*: 'Coordinated multipoint: concepts, performance, and field trial results', *IEEE Commun. Mag.*, 2011, **49**, (2), pp. 102–111

10 Costa, M.H.M.: 'Writing on dirty paper', *IEEE Trans. Inf. Theory*, 1983, **29**, (3), pp. 439–441

11 Yu, W., Ginis, G., Cioffi, J.M.: 'Distributed multiuser power control for digital subscriber lines', *IEEE Trans. J. Sel. Areas Commun.*, 2002, **20**, (5), pp. 1105–1115

12 Kobayashi, M., Caire, G.: 'Iterative waterfilling for weighted rate sum maximization in MIMO-OFDM broadcast channels'. IEEE Int. Conf. Acoustics, Speech, Signal Processing (ICASSP), Honolulu, HI, USA, April 2007

13 Zheng, G., Wong, K.-K., Ng, T.-S.: 'Throughput maximization in linear multiuser MIMO-OFDM downlink systems', *IEEE Trans. Veh. Technol.*, 2008, **57**, pp. 1993–1998

14 Il Shin, Y., Kang, T.-S., Kim, H.-M.: 'An efficient resource allocation for multiuser MIMO-OFDM systems with zero-forcing beamformer'. IEEE Int. Symp. Personal, Indoor, Mobile Radio Communications (PIMRC), Athens, Greece, September 2007

15 Holakouei, R., ao Silva, A., Gameiro, A.: 'Distributed versus centralized zero-forcing precoding for multicell OFDM systems'. IEEE Global Telecommunications Conf. Workshops (GLOBECOM), Houston, TX, USA, December 2011

16 Kaviani, S., Krzymie?, W.A.: 'User selection for multiple-antenna broadcast channel with zero-forcing beamforming'. IEEE Global Telecommunications Conf. (GLOBECOM), New Orleans, LO, USA, December 2008

17 Papandriopoulos, J., Evans, J.S.: 'SCALE: A low-complexity distributed protocol for spectrum balance in multiuser DSL networks', *IEEE Trans. Inf. Theory*, 2009, **8**, (8), pp. 3711–3724

18 Hassan, N.U., Assaad, M.: 'Optimal downlink beamforming and resource allocation in MIMO-OFDMA systems'. IEEE Int. Workshop Signal Processing Advanced Wireless Communications (SPAWC), Marrakech, Morocco, June 2011

19 Venturino, L., Prasad, N., Wang, X.: 'Coordinated scheduling and power allocation in downlink multicell OFDMA networks', *IEEE Trans. Veh. Technol.*, 2009, **6**, (58), pp. 2835–2848

20 Boyd, S., Vandenberghe, L.: 'Convex optimization' (Cambridge University Press, Cambridge, UK, 2004)

21 Anderson, H.R.: 'Fixed broadband wireless system design' (John Wiley & Sons Ltd., UK, 2003)

22 Goldsmith, A.: 'Wireless communications' (Cambridge University Press, New York, USA, 2005)

23 Stüber, G.L., Barry, J., McLaughlin, S.W., Li, Y.G., Ingram, M.A., Pratt, T.G.: 'Broadband MIMO-OFDM wireless communication'. Proc. of IEEE, February 2004, vol. 92, pp. 271–294

24 Horst, R., Tuy, H.: 'Global optimization: deterministic approaches' (Springer-Verlag, Berlin, Germany, 1993, 2nd edn.)

25 Holma, H., Toskala, A. (EDs.): 'WCDMA for UMTS – HSPA evolution and LTE' (John Wiley & Sons Ltd., West Sussex, UK, 2007, 4th edn.)

26 Holma, H., Toskala, A. (EDs.): 'LTE for UMTS: OFDMA and SC-FDMA based radio access' (John Wiley & Sons Ltd., West Sussex, UK, 2009)

27 Prabhu, R.S., Daneshrad, B.: 'An energy-efficient water-filling algorithm for OFDM systems'. IEEE Int. Conf. Communications (ICC), Cape Town, South Africa, May 2010